Organic Electronics 15 (2014) 2639–2646

Contents lists available at ScienceDirect

Organic Electronics

journal homepage: www.elsevier.com/locate/orgel

Using unsorted single-wall carbon nanotubes to enhance mobility of diketopyrrolopyrrole-quarterthiophene copolymer in thin-film transistors

Chad Smithson [a,b], Yiliang Wu [b,*], Tony Wigglesworth [b], Sandra Gardner [b], Shiping Zhu [a,*], Heng-Yong Nie [c]

[a] Department of Chemical Engineering, McMaster University, 1280 Main Street West, Hamilton, ON L8S 4L8, Canada
[b] Advanced Materials Laboratory, Xerox Research Centre of Canada, 2660 Speakman Dr., Mississauga, ON L5K 2L1, Canada
[c] Surface Science Western, The University of Western Ontario, 999 Collip Circle, London, ON N6G 0J3, Canada

ARTICLE INFO

Article history:
Received 20 May 2014
Received in revised form 9 July 2014
Accepted 13 July 2014
Available online 5 August 2014

Keywords:
Organic thin-film transistors
Single-wall carbon nanotubes
Diketopyrrolepyrrole–quarterthiophene copolymer
Field effect mobility
Current on/off ratio

ABSTRACT

Organic thin film transistors (OTFTs) were fabricated for the first time using a semiconductor copolymer of diketopyrrolopyrrole-quarterthiophene (DPP-QT) and unsorted single walled carbon nanotubes (SWCNTs). Three different SWCNTs having different tube diameters, length, and shape were used to investigate the effects of carbon nanotubes' properties on dispersion of the SWCNTs in DPP-QT polymer, as well as the mobility and current on/off ratio of the OTFTs. The DPP-QT polymer was able to selectively disperse two types of SWCNTs. An optimal SWCNT loading was found to be 1.5–2.5 wt% for these SWCNTs, before the on/off ratio fell below 10^5 due to increased metallic tube content of the film. At this optimal loading, the field effect mobility was improved by a factor of two, with the maximum mobility reaching 1.3 $cm^2 V^{-1} s^{-1}$, when the SWCNTs with a short length and small tube diameter were used.

© 2014 Elsevier B.V. All rights reserved.

1. Introduction

A major goal for printable electronic devices is the development of organic thin-film transistors (OTFTs) [1–3]. By replacing the brittle silicon based semiconductor with an organic semiconductor material, new opportunities for low-cost, flexible, and lightweight electronics exist, since an organic semiconductor could be integrated into large area electronic device via printing techniques in a roll to roll manner [4]. One of the most challenging aspects to this approach is generating a cost effective semiconductor materials with comparable electrical performance to amorphous silicon which has a mobility of 0.5–1 $cm^2 V^{-1} s^{-1}$. Over the past 10 years, a wealth of research has been published using single walled carbon nanotubes (SWCNTs) to generate high mobility films due to their high field effect mobility measured to be 79,000 $cm^2 V^{-1} s^{-1}$ and an intrinsic mobility estimated at 100,000 $cm^2 V^{-1} s^{-1}$ [5]. SWCNTs can be incorporated into the semiconductor layer of existing OTFT designs making them an ideal candidate for technology development [6]. Research into individual SWCNT channels grown by chemical vapour deposition (CVD) have been reported [7–10], but these methods suffer from their inability to be scaled to production demands. Success has been made depositing filtered films of SWCNTs, but the process still requires multiple steps, making it labour intensive [11,12]. Due to their tendency to aggregate in solution, a film of pure CNTs cannot be solution cast without the aid of a dispersing agent, which can affect film

* Corresponding authors. Tel.: +1 (905) 823 7091x448; fax: +1 905 822 7022 (Y. Wu). Tel.: +1 (905) 525 9140x24962 (S. Zhu).
E-mail addresses: yiliang.wu@xrcc.xeroxlabs.com (Y. Wu), zhuship@mcmaster.ca (S. Zhu).

http://dx.doi.org/10.1016/j.orgel.2014.07.021
1566-1199/© 2014 Elsevier B.V. All rights reserved.

Table 1
Unsorted SWCNTs and their properties used in this study.

Sample ID	Diameter (nm)	Length (mm)	Metal catalyst	Cleaning method
CNT-A	0.7–0.9	0.5–2	CoMoCAT®	HF (aq) wash
CNT-B	0.7–2.5	0.5–5	HipCo	Hydroxyl wash
CNT-C	1–2	3–30	Co	Plasma purified

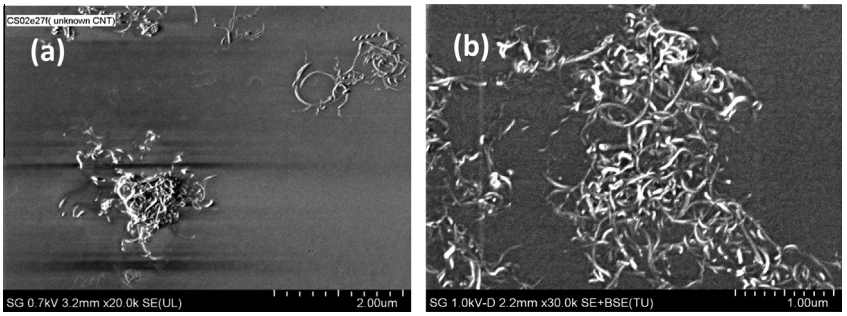

Fig. 1. (a) SEM images of CNT-B spin coated on SiO_2 wafer (scale 2 μm). (b) DPP-QT film with a maximum loading of CNT-B (scale 1 μm).

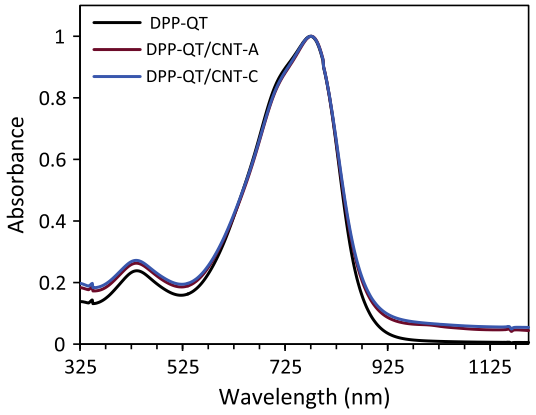

Fig. 2. Solution UV–Vis spectra. All solutions contain 0.5 wt% DPP-QT polymer in 1,1,2,2-tetrachloroethane with DPP-QT/CNT-A containing 5 wt% CNT-A by solids and DPP-QT/CNT-C containing 5 wt% CNT-C by solids.

preparation and SWCNT performance [13–15]. It has been shown that oxidized or chemically functionalized CNT's are more easily dispersed in solvents than defect free CNT's [16]. However, these methods are not useful for semiconductor electronics, because altering the chemical structure of a CNT diminishes its semiconductor properties.

An alternative approach to generating a pure film of SWCNTs is to use SWCNTs to enhance the performance of organic semiconductors. Due to their high aspect ratio, a very small amount of SWCNTs can be added to a semiconductor polymer film increasing the films overall mobility [17]. This approach requires the semiconductor to be soluble and able to stabilize a dispersed SWCNT solution. Fortunately most semiconductor polymers consist of a conjugated backbone, allowing for a π–π interaction to help prevent the aggregation of CNTs in solution. One of

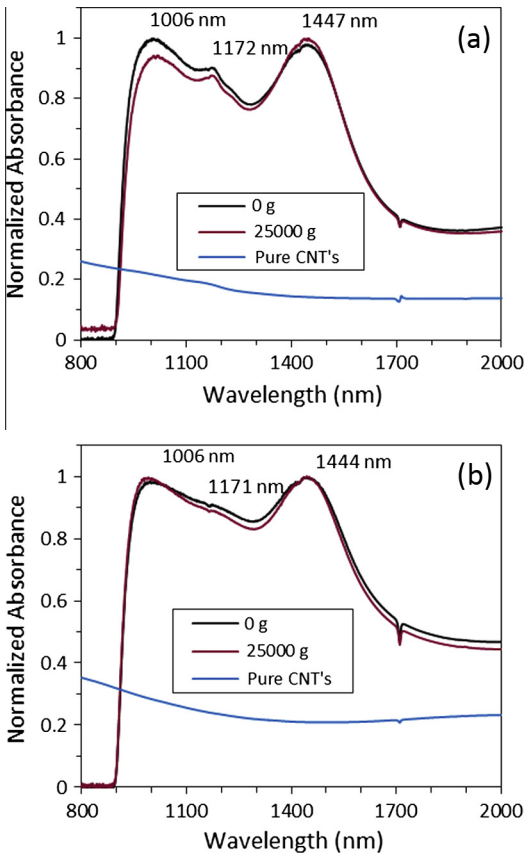

Fig. 3. UV–Vis spectra of 0.5 wt% DPP-QT polymer in 1,1,2,2-tetrachloroethane solution with 5 wt% (a) CNT-A and (b) CNT-C of the total solutes, before and after centrifuging at 25,000 g for 30 min. The spectra of a dispersion of the same amount of SWCNTs without the polymer were also included.

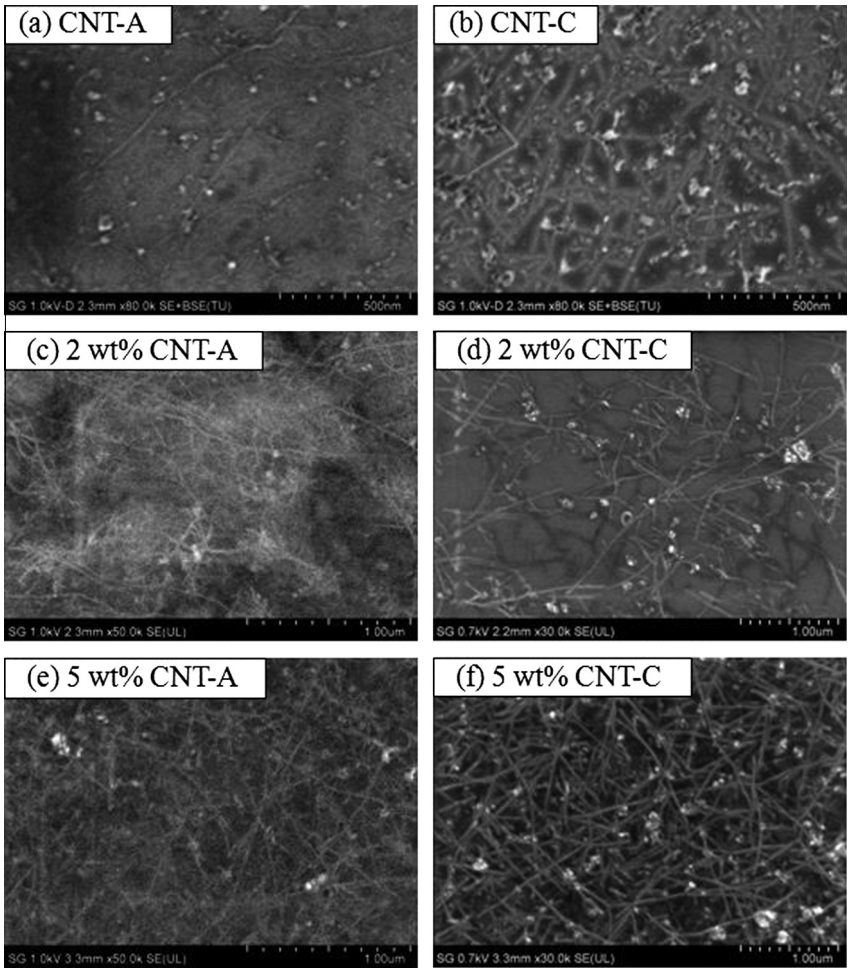

Fig. 4. SEM images of CNT films cast on OTS modified silicon wafers. (a), (c), (e) are CNT-A and (b), (d), (f) are CNT-C. Images (a) and (b) are films cast from a freshly sonicated solution containing pure CNTs, while (c–f) are films with an indicated CNT content, in a film of DPP-QT copolymer. Amorphous carbon impurities can be observed as round bright spots in the film. The CNTs were well dispersed with no noticeable aggregates.

Table 2
Average CNT density determined from a visual count of the SEM images.

CNT loading (wt%)	CNT-A (tubes μm^{-2})	CNT-C (tubes μm^{-2})
2	11.3	9.2
5	20.9	19.6

the most studied semiconductors polymers employing this approach is poly(3-alkythiophene) [18–20]. Although mobility improvements up to 10 times have been reported [21], due to the low mobility of poly(3-alkythiophene), the absolute mobility values are still very low, for example less than 0.1 $cm^2 V^{-1} s^{-1}$. Recently a new class of semiconductor, diketopyrrolopyrrole-quarterthiophene copolymer with mobility up to 1.0 $cm^2 V^{-1} s^{-1}$, has been reported. It would be interesting to study if the mobility can be further enhanced by using SWCNTs as additive.

A major challenge with SWCNTs is that when synthesized, they are generated as a mixture of approximately 1/3 metallic carbon nanotubes (*m*-CNT) and 2/3 semiconducting carbon nanotubes (*sc*-CNT) [9]. The presence of metallic tubes is detrimental for OTFTs because beyond the percolation threshold they can create a conductive pathway essentially short circuiting the device. Additionally they have been found to reduce the on/off ratio of OTFTs [12]. To avoid the detrimental effects caused by *m*-CNTs, SWCNTs are semiconductor enriched. Three major techniques are employed for semiconductor enrichment to separate *m*-CNTs from *sc*-CNTs. Density gradient ultracentrifugation (DGU) has achieved the best purity, but has very small throughput ~1 mg every 48 h [22–28]. Other methods such as column chromatography [29,30], selective oxidation [31] or separation employing SWCNT selective polymers [32,33] offer higher throughput but are still well below commercial requirements. Most literature employing SWCNT films utilizes these semiconductor enriched SWCNTs [14,34–36]. The challenge with this approach is that the cost to purify these tubes drives the cost of materials so high that an amorphous silicon film remains a cheaper option.

Instead of using high-cost purified SWCNTs we looked into the cheaper alternative of using unsorted SWCNTs.

The focus of this research was to determine if this mixture of metallic and semiconducting tubes could be used as a viable option for mobility enhancement of the new semiconductor copolymer of diketopyrrolopyrrole-quarterthiophene, and if so, what physical properties of the unsorted SWCNTs are best for this application.

2. Results and discussion

2.1. Materials

Three sources of SWCNT were studied in this report, one from Sigma Aldrich which will be abbreviated CNT-A, one from BuckyUSA abbreviated CNT-B and one from Cheap Tubes abbreviated CNT-C. These sources were chosen because these SWCNTs have different tube diameters, length, surface finish, etc. Full descriptions of the SWCNTs can be found in Table 1. CNT-A has short average tube length and the smallest tube diameter, CNT-B has shorter tube length comparable to CNT-A, but larger variation in tube diameter, while CNT-C has the longest tube length of 3–30 μm, and larger tube diameter. In addition they were all prepared using combustion chemical vapour deposition (CCVD) but were purified by different methods.

The semiconductor diketopyrrolopyrrole-quarterthiophene copolymer (DPP-QT) with a reported mobility of 1 $cm^2 V^{-1} s^{-1}$ [1,2], but an average mobility of 0.6 $cm^2 V^{-1} s^{-1}$ as measured in our lab was chosen to form the bulk of the semiconductor film, as this polymer has a high baseline mobility. By dissolving the copolymer in 1,1,2,2-tetrachloroethane and adding SWCNTs, the SWCNT aggregates could be dispersed by using an ultrasonic probe for 2 min. The dispersion of SWCNTs in DPP-QT copolymer was then spin coated to generate a semiconductor film and further integrated into OTFTs. The dispersion of SWCNTs in the film, as well as their effect on electrical performance of OTFTs was examined.

2.2. Dispersion and thin film characterization

Our previous research into SWCNT dispersions was performed using the Poly[5,5′-bis(3-dodecyl-2-thienyl)-2,2′-bithiophene] (PQT-12) and HipCo SWCNTs from BuckyUSA (CNT-B in this study). It has been shown that this SWCNT could be dispersed very well in PQT-12 at high carbon nanotube loading [37]. When the same source SWCNTs were used with the DPP-QT polymer, very few SWCNTs could be stabilized in solution. A modest centrifugation for 15 min at 2050 g appeared to remove almost all the SWCNTs from solution. However, SEM images of films cast from DPP-QT and CNT-B revealed areas of high CNT aggregation and others with no CNT content (Fig. 1). Because most of the tubes were centrifuged out of the sample, the SWCNT concentration was unknown. All initial SWCNT loading concentrations tested (1–15 wt%), produced roughly the same mobility of 0.97 $cm^2 V^{-1} s^{-1}$ and on/off ratio of 4×10^7 in OTFTs, suggesting a maximum loading of less than 1 wt%. The improvement caused by the tubes corresponds to a film mobility improvement of 50%, but did not offer the opportunity for further study of SWCNT concentration effects. For this reason we looked to other types of SWCNTs and found excellent stabilization of SWCNTs when the sources were CNT-A and CNT-C. The dispersion was stable for up to a few weeks without forming any agglomeration. Interestingly PQT-12 was unable to stabilize these two SWCNTs in any appreciable amount.

Previous reports have shown that for similar polymers such as the PQT polymer, a blue shift and broadening is observed in the Ultraviolet–Visible spectrum (UV–Vis) due to a π–π interaction caused by the polymer wrapping around the CNTs [37,38]. Fig. 2 provides UV–Vis data with the black line representing a 0.5 wt% solution of DPP-QT copolymer in 1,1,2,2-tetrachloroethane, while the red and blue curves show the same 0.5 wt% solution with 0.025 wt% CNT-A and CNT-C respectively. These CNT values correspond to 5 wt% solids in solution. There is no peak shifting or line broadening in the UV–Vis, indicating little interaction between the polymer and CNT's in the solution phase.

Although there is no shifting of the UV–Vis peaks suggesting no significant π–π interaction between DPP-QT and CNTs, the copolymer did stabilize the CNTs in solution for a minimum of 2 weeks. Fig. 3 shows an undiluted UV–Vis sample. When no polymer is present to stabilize the CNTs (blue[1] line), no distinct features are observed and the CNTs can clearly be seen to aggregate within minutes suggesting there is little to no CNTs in solution. However, we observe a CNT signal for the S_{22} band with a maximum at 1006 nm corresponding to a 6,5 chirality [39], a shoulder at 1172 nm corresponding to the 7,6 or 9,2 chirality [40], and the S_{11} band with a maximum at 1447 nm corresponding to the 10,8 chirality [41], when the DPP-QT polymer was present. It is common practice when working with CNTs to centrifuge the aggregates out of solution. To determine if this was necessary, samples were probe sonicated at 35% amplitude for 2 min and centrifuged at 25,000 g for 30 min. No significant change in peak intensity was observed and no visible sign of a precipitate could be observed in the vial, indicating no material was removed during centrifugation. For this reason, all other samples in this report were not centrifuged. The above results indicated that DPP-QT polymer could stabilize these two types of CNTs, but had no selectivity in carbon nanotube chirality.

From the above results it is clear that the CNT-A and CNT-C are being stabilized in solution. To investigate their dispersion, we referred to SEM imaging of a 100 nm spin coated film (Fig. 4). Due to the high conductivity of the *m*-CNTs and *sc*-CNTs, they require no conductive coating and image much more easily than the copolymer. This provides excellent contrast between the CNT's and copolymer. It should be noted that in all the images the bright spots are amorphous carbon. To produce a film without polymer present, the CNTs had to be spin coated immediately after being probe sonicated. The pure SWCNT films (a) and (b) display poor coverage where most of the SWCNTs did not adhere to the surface during spin coating. Images (c–f) show well dispersed CNTs embedded in the polymer

[1] For interpretation of color in Fig. 3, the reader is referred to the web version of this article.

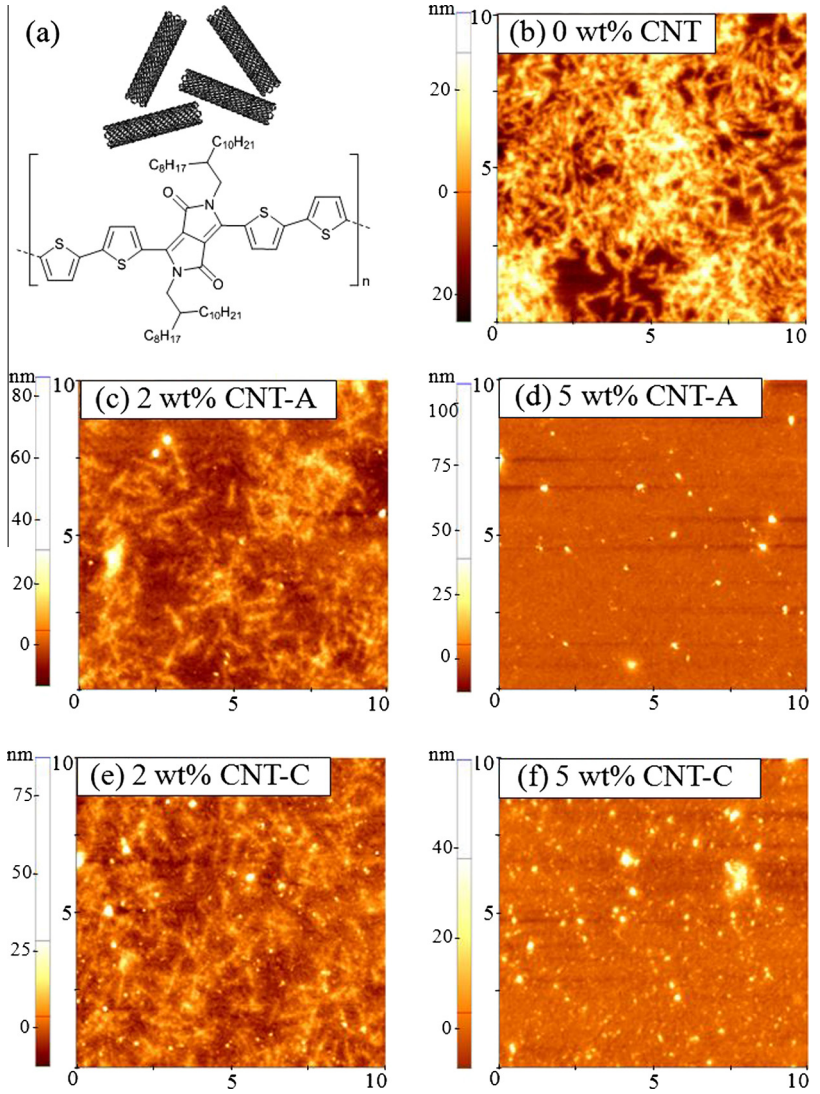

Fig. 5. AFM images (scan area: 10 μm × 10 μm) of films cast on OTS modified wafers. All films are primarily composed of DPP-QT polymer with varying CNT contents. The images correspond to (b) 0 wt%, (c) 2 wt%, and (d) 5 wt% CNT-A, respectively; (e) 2 wt% and (f) 5 wt% CNT-C, respectively. Polymer crystal domains are seen to shrink in size with increasing CNT content demonstrating the interruption of the CNTs have on the polymer crystal packing.

matrix. As expected the CNT density increases with increasing CNT loading in the dispersion. Performing a visual count of the CNTs in each image, an average CNT density was determined for each CNT wt%. The results are summarized in Table 2. In contrast, CNT-B was found to have a low loading capacity and formed aggregates in the film (Fig. 1). This is likely due to the hydroxyl washing used to purify CNT-B which can alter the chemical surface of the SWCNTs.

After observing the excellent dispersion of SWCNT in the film, we looked at how these affected film morphology of the polymer. Atomic force microscopy (AFM) images of the pure DPP-QT film reveal polycrystalline domains of approximately 0.2–1 μm in size. These organized domains are important for achieving high mobility devices. However, as the SWCNTs were introduced, there is a noticeable decrease in the polycrystalline domain size of the polymer. At 5 wt% CNT content, the polycrystalline domains have been reduced to the nanoscale (Fig. 5). There are two major ways the CNTs were thought to interact with the polymer. The average radius of a SWCNT is 1 nm, allowing it to insert itself between two layers of a crystalline polymer. If this were to occur, the average *d*-space between the polymer chains would change, creating a shift in the XRD signal. The other option is that the CNTs would completely interrupt the crystalline packing of the polymer, reducing the size of the polycrystalline domains. This is confirmed by the lack of shifting in the XRD spectra seen in Fig. 6. The peak at 5.26° corresponds to the interlayer spacing of the polymer (between side chains) [1]. The intensity of the peaks cannot be used as a measure of polycrystallinity due to the low angle required during sample collection generating a large amount of background noise. The observation is consistent with previous reports on systems containing CNTs and other semiconductor polymers [4,37].

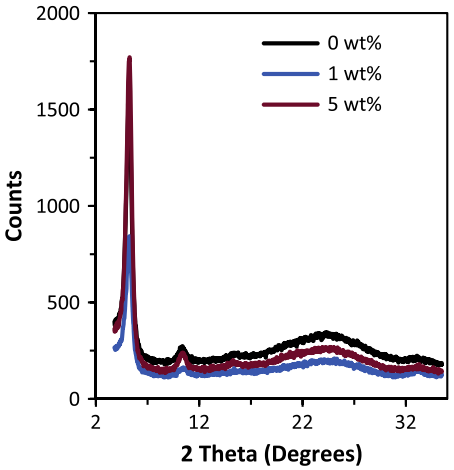

Fig. 6. XRD of the DPP-QT/CNT-A film shows no interaction of CNTs with polymer crystals. No shifting of the main peak suggesting the CNTs are not being inserted between polymer layers, but are interrupting the packing of the crystal network, causing smaller crystal domains.

2.3. Electronic characteristics

OTFT devices were fabricated using varying concentrations of CNT-A and CNT-C. Fig. 7 provides a typical set of data for the I_{SD} vs V_{SG} transfer curves. With increasing CNT concentration, a noticeable decrease in the on/off ratio is observed. This is consistent with other literature findings and is largely due to the high metallic CNT content of the sample [12,42]. Additionally we observe a reduced turn on voltage corresponding to a shifted threshold voltage V_T when the SWCNT concentration is increased. This is due to a reduced charge injection resistance caused by the SWCNTs. Results of this were further explored using 3 different metal electrodes (Au, Cu, Al) where the results are summarized in our previous article [43].

To determine an optimal loading of the unsorted SWCNTs, a series of SWCNT concentrations was measured from 0 to 5 wt%. All data points are a statistical average with a minimum of 8 data points measured for each concentration. Error bars are given for one standard deviation. Referring to Fig. 8, it is clear that the addition of unsorted SWCNTs has an enhancing effect on the mobility of the DPP-QT/SWCNT film. Despite their interruption of the polycrystalline domains in the film, an increase in mobility is still observed when SWCNT's are added to the film. Both CNT-A and CNT-C show an increase in mobility reaching a maximum at 2.5 and 2.0 wt%, respectively. The decrease preceding these maximum is caused by the onset of percolation of the *m*-SWCNTs. The increasing addition of *m*-SWCNTs has a nearly exponential decrease in the on/off ratio of the film. At 5 wt% SWCNT, the film has nearly reached the percolation limit, providing pathways from source to drain consisting primarily of *m*-CNTs generating a short circuited device. Interestingly, reports of films formed from pure SWCNT films hit the percolation limit at a smaller SWCNT density of only 3 CNTs/μ^2 as opposed to the 20 tubes/μ^2 required in this report. From this we can conclude that the separation between SWCNTs caused by the polymeric matrix allows for a larger loading of unsorted SWCNTs before percolation is achieved [44]. For commercial use, these devices require a minimum on/off limit of 10^5, which sets an upper limit to how many unsorted SWCNTs can be added. For these two CNT sources, the average mobility with a current on/off ratio over 10^5 was 1.1 and 0.72 $cm^2\ V^{-1}\ s^{-1}$, corresponding to an optimal loading concentration of 2.5 wt% and 1.5 wt% for CNT-A and CNT-C, respectively. The maximum mobility for DPP-QT/CNT-A composition was up to 1.3 $cm^2\ V^{-1}\ s^{-1}$. The loading of CNT-A is larger than CNT-C likely because the CNT-A tubes have a shorter tube length and a higher aspect ratio. These results show that although both CNT types can be dispersed in the polymer matrix at variable concentrations, but their mobility enhancement is different. CNT-C has a large decrease in on/off ratio even at low concentrations, showing that long tubes allow percolation of *m*-CNTs faster than short tubes. The impact of the long *m*-CNTs is so detrimental to device performance that CNT-C has almost no positive impact on electrical performance. Therefore we conclude that if one is to use

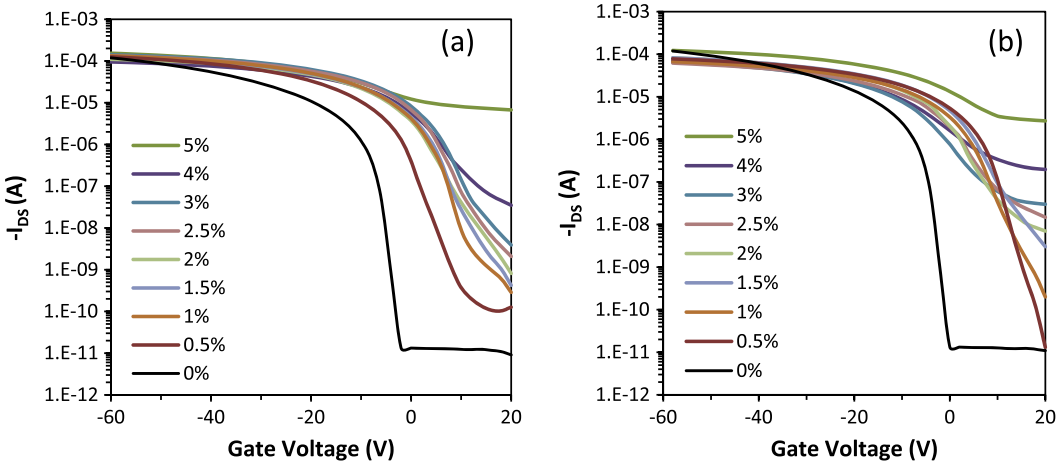

Fig. 7. Transfer curves for the DPP-QT polymer with various amounts of CNT-A (a) and CNT-C (b) added by wt% to the film.

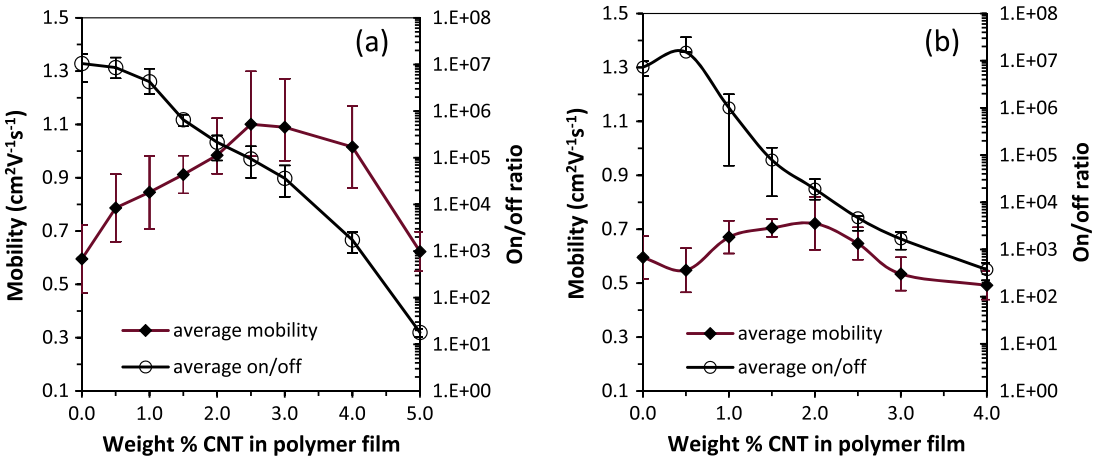

Fig. 8. Mobility and on/off ratio for DPP-QT/CNT-A blend (a) and DPP-QT/CNT-C blend (b). A maximum mobility was obtained at 2.5 and 2.0 wt% CNT for these two films. The on/off ratio was found to decrease in an exponential fashion corresponding to increasing CNT concentration. The error bars represent the spread of data, with the data points being an average value.

unsorted SWCNTs for mobility enhancement, shorter CNTs are ideal because *m*-CNT percolation occurs at higher concentrations. Another consequence of the addition of unsorted SWCNTs is the shift of the threshold voltage. The DPP-QT polymer has an average threshold voltage around −4.0 V. Upon addition of CNTs, the threshold voltages shifted to 6.4 and 6.6 V at 0.5 wt% CNT loading, and subsequently stabilized at around 8.0 and 7.0 V at a higher loading for CNT-A and CNT-C, respectively. Although the threshold voltage shift has a negative impact on the DPP-QT polymer, it could be useful for other semiconductor devices that have a large negative threshold voltages [45–47] to shift the value close to 0 V. The increased threshold voltage also caused the subthreshold slope to decrease from 0.67 dec/V for the pure DPP-QT device to about 0.2 dec/V the DPP-QT/CNT devices having the maximum mobility values.

3. Conclusion

We have demonstrated that three types of unsorted SWCNTs can be stabilized by the DPP-QT polymer in a 1,1,2,2-tetrachloroethane solution. The CNT-B source was found to have a low loading capacity, likely due to the hydroxyl washing used to purify the tubes. CNT-A and CNT-C which are not chemically altered during purification were easily dispersed and stabilized by the DPP-QT copolymer. Morphologies of the films showed that the CNT-A and CNT-C were evenly dispersed in the DPP-QT with no large aggregates, while CNT-B formed large aggregated clusters in the film. AFM and XRD measurements indicated that the CNTs interrupt the polycrystalline domains. Smaller polycrystalline domains were observed at higher CNT concentrations. The commercial source of SWCNTs which relates back to SWCNT length, thickness, and cleaning methods, plays an important role in the interaction of the SWCNT with the semiconductor polymer. These dispersions can be spin coated into films on an OTS modified silicon wafer and annealed at 140 °C to form semiconductor films for OTFTs. The addition of unsorted SWCNTs, consisting of a mixture of approximately 2/3 *sc*-SWCNT and 1/3 *m*-SWCNTs, allowed for mobility enhancement. Maximum loading concentrations for CNT-A and CNT-C were found to be 2.5 wt% and 1.5 wt%, respectively, beyond which the on/off ratio falls below 10^5. The CNTs (CNT-C) with relatively longer length reach percolation at a lower concentration, causing a quick reduction of the on/off ratio. The CNTs (CNT-A) with the relatively shorter length and smaller tube diameter provide the greatest mobility enhancement, approximately doubling the mobility of the pure DPP-QT polymer device.

4. Experimental section

4.1. Materials and general methods

All solvents were reagent grade purchased from Sigma Aldrich and used as received. CNT-A was purchased from Sigma Aldrich (704,148) (6,5) chirality, carbon >90%, 77% (carbon as SWCNT), 0.7–0.9 nm diameter, 0.5 – 2 μm length; CNT-B was obtained from Bucky USA BU-203 – OH Hydroxy 95 wt%, 0.7–2.5 nm diameter, 0.5–5 μm length; and CNT-C was purchased from Cheap Tubes (SKU-0111) SW/DWCNTs, >99 wt%, 1–2 nm diameter, 3–30 μm length.

DPP-QT was synthesized following the procedure reported by Choi et al. [2]. Diketopyrrolopyrrole-quaterthiophene copolymer (DPP-QT) (0.02 g) was dissolved in 1,1,2,2-tetrachlorethane (3.98 g) for 2 h at 80 °C in the absence of light to form a 0.5 wt% solution. 1.5 mg, of SWCNTs was added to 5.699 g of 0.5 wt% DPP-QT solution. The solution was immersed in an ice bath and probe sonicated on a Branson Digital Sonifier-450 (400 W) at 35% amplitude for 2 min. The resultant solution was a 0.5 wt% solution with a 5 wt% CNT concentration with respect to the polymer weight. All subsequent solutions were created via dilution by adding additional 0.5 wt% DPP-QT solution. For DPP-QT/CNT-B composition, the resultant dark green

solution was centrifuged at 2054 g for 15 min and the supernatant collected. The resultant solution was a 0.5 wt% DPP-QT polymer with an unknown CNT concentration.

For SEM, samples were imaged in their native condition (no conductive coating applied) using a Hitachi SU-8000 field emission scanning electron microscope (SEM) operating in deceleration mode with a landing voltage of 700 V. A Park Systems XE-100 AFM operated in dynamic force mode was used to obtain AFM images. A cantilever with a nominal spring constant of 40 N/m, a resonant frequency of 300 kHz and a probe having a radius of 10 nm was used. Each sample had 2–3 spots imaged at each scan size with the most representative image presented in this report. UV–Visible spectra were collected on a Varian Cary UV–Vis-IR Spectrometer. Data in the 325–1150 nm range was collected using a 1 cm cell with a solution diluted to 0.004 wt% DPP-QT. Data in the 800–2000 nm range was collected using a 1 mm cell and an undiluted sample with an undiluted DPP-QT background used for the 0 g and 25,000 g samples. X-ray diffractions (XRD) were obtained using a Co source (D8 Discover) knife edge experiment, 1° incidence, 19.934 cm detector distance, 2 h collection time.

4.2. OTFT fabrication and evaluation

All fabrication and characterization of organic thin-film transistor devices (OTFTs) was done under ambient conditions taking precautions to isolate the material and device from light, but no precautions were taken to isolate the material or device from exposure to air or moisture. Bottom-gate TFT devices were built on n-doped silicon wafer as the gate electrode with a 110 nm thermal silicon oxide (SiO_2) as the dielectric layer. The SiO_2 surface was plasma cleaned for 2 min. The wafer was subsequently rinsed with H_2O than isopropanol and dried with an air stream. The SiO_2 surface was modified with octyltrichlorosilane (OTS-8) by immersing a cleaned silicon wafer substrate in 0.1 M OTS-8 in toluene at 60 °C for 20 min. The wafer was subsequently rinsed with toluene and isopropanol and dried with an air stream. The semiconductor layer was deposited onto the OTS-8-modified SiO_2 layer by coating one of the above prepared solutions and allowing it to sit on the wafer for 2 min, then spin coating with a 2 s ramp time, at 2000 rpm for 120 s. The sample was vacuum dried at 70 °C for 30 min and annealed at 140 °C for 40 min, and allowed to return to room temperature under vacuum. Subsequently, the gold source and drain electrodes were deposited by vacuum evaporation through a shadow mask with a channel length (L) of 90 μm and a width (W) of 1 mm.

From I_D–V_G measurements, the mobility was extracted from the saturated regime using the following equation ($V_D > V_G$):

$I_D = C_i\mu(W/2L)(V_G - V_T)^2$, where I_D is the drain current, C_i is the capacitance per unit area of the gate dielectric layer, V_G and V_T are the gate voltage and threshold voltage, respectively.

References

[1] Y. Li, P. Sonar, S.P. Singh, M.S. Soh, M. van Meurs, J. Tan, J. Am. Chem. Soc. 133 (2011) 2198.
[2] J.S. Ha, K.H. Kim, D.H. Choi, J. Am. Chem. Soc. 133 (2011) 10364.
[3] J. Li, Y. Zhao, H.S. Tan, Y. Guo, C.-A. Di, G. Yu, Y. Liu, M. Lin, S.H. Lim, Y. Zhou, H. Su, B.S. Ong, Sci. Rep. 2 (2012) 754.
[4] G.-W. Hsieh, F.M. Li, P. Beecher, A. Nathan, Y. Wu, B.S. Ong, W.I. Milne, J. Appl. Phys. 106 (2009) 123706.
[5] T. Dürkop, S.A. Getty, E. Cobas, M.S. Fuhrer, Nano Lett. 4 (2004) 35–39.
[6] Q. Cao, J.A. Rogers, Adv. Mater. 21 (2009) 29.
[7] M.S. Fuhrer, B.M. Kim, T. Dürkop, T. Brintlinger, Nano Lett. 2 (2002) 755.
[8] S.J. Tans, A.R.M. Verschueren, C. Dekker, Nature 393 (1998) 49.
[9] C. Rutherglen, D. Jain, P. Burke, Nat. Nanotechnol. 4 (2009) 811.
[10] C. Kocabas, N. Pimparkar, O. Yesilyurt, S.J. Kang, M. A Alam, J.A. Rogers, Nano Lett. 7 (2007) 1195.
[11] M.Y. Timmermans, D. Estrada, A.G. Nasibulin, J.D. Wood, A. Behnam, D. Sun, Y. Ohno, J.W. Lyding, A. Hassanien, E. Pop, E.I. Kauppinen, Nano Res. 5 (2012) 307.
[12] D. Sun, M.Y. Timmermans, Y. Tian, A.G. Nasibulin, E.I. Kauppinen, S. Kishimoto, T. Mizutani, Y. Ohno, Nat. Nanotechnol. 6 (2011) 156.
[13] Z. Wu, Z. Chen, X. Du, J.M. Logan, J. Sippel, M. Nikolou, K. Kamaras, J.R. Reynolds, D.B. Tanner, A.F. Hebard, A.G. Rinzler, Science 305 (2004) 1273.
[14] N. Rouhi, D. Jain, K. Zand, P.J. Burke, Adv. Mater. 23 (2011) 94.
[15] M.D. Lay, J.P. Novak, E.S. Snow, Nano Lett. 4 (2004) 603.
[16] D.S. Kim, D. Nepal, K.E. Geckeler, Small 1 (2005) 1117.
[17] J. Zou, L. Liu, H. Chen, S.I. Khondaker, R.D. McCullough, Q. Huo, L. Zhai, Adv. Mater. 20 (2008) 2055.
[18] A. Ikeda, K. Nobusawa, T. Hamano, J. Kikuchi, Org. Lett. 8 (2006) 5489.
[19] M. Giulianini, E.R. Waclawik, J.M. Bell, M. De Crescenzi, P. Castrucci, M. Scarselli, N. Motta, Appl. Phys. Lett. 95 (2009) 013304.
[20] H.W. Lee, Y. Yoon, S. Park, J.H. Oh, S. Hong, L.S. Liyanage, H. Wang, S. Morishita, N. Patil, Y.J. Park, J.J. Park, A. Spakowitz, G. Galli, F. Gygi, P.H.-S. Wong, J.B.-H. Tok, J.M. Kim, Z. Bao, Nat. Commun. 2 (2011) 1.
[21] Y.J. Song, J.U. Lee, W.H. Jo, Carbon 48 (2010) 389.
[22] Y. Feng, Y. Miyata, K. Matsuishi, H. Kataura, J. Phys. Chem. C 115 (2011) 1752.
[23] V.K. Sangwan, R.P. Ortiz, J.M.P. Alaboson, J.D. Emery, M.J. Bedzyk, L.J. Lauhon, T.J. Marks, M.C. Hersam, ACS Nano 6 (2012) 7480.
[24] M.S. Arnold, A. A Green, J.F. Hulvat, S.I. Stupp, M.C. Hersam, Nat. Nanotechnol. 1 (2006) 60.
[25] J.A. Fagan, M.L. Becker, J. Chun, E.K. Hobbie, Adv. Mater. 20 (2008) 1609.
[26] S. Ghosh, S.M. Bachilo, R.B. Weisman, Nat. Nanotechnol. 5 (2010) 443.
[27] M.S. Arnold, S.I. Stupp, M.C. Hersam, Nano Lett. 5 (2005) 713.
[28] A.A. Green, M.C. Hersam, Adv. Mater. 23 (2011) 2185.
[29] T. Tanaka, Y. Urabe, D. Nishide, H. Kataura, Appl. Phys. Express 2 (2009) 125002.
[30] T. Tanaka, H. Jin, Y. Miyata, S. Fujii, H. Suga, Y. Naitoh, T. Minari, T. Miyadera, K. Tsukagoshi, H. Kataura, Nano Lett. 9 (2009) 1497.
[31] Y. Miyata, Y. Maniwa, H. Kataura, J. Phys. Chem. B 110 (2006) 25.
[32] K.S. Mistry, B.A. Larsen, J.L. Blackburn, ACS Nano 7 (2013) 2231.
[33] A. Nish, J.-Y. Hwang, J. Doig, R.J. Nicholas, Nat. Nanotechnol. 2 (2007) 640.
[34] S.D. Stranks, S.N. Habisreutinger, B. Dirks, R.J. Nicholas, Adv. Mater. 25 (2013) 1.
[35] C. Wang, J. Zhang, K. Ryu, A. Badmaev, L.G. De Arco, C. Zhou, Nano Lett. 9 (2009) 4285.
[36] M. Engel, J.P. Small, M. Steiner, M. Freitag, A.A. Green, M.C. Hersam, P. Avouris, ACS Nano 2 (2008) 2445.
[37] C. Derry, Y. Wu, S. Zhu, J. Deen, J. Electron. Mater. 42 (2013) 3481.
[38] A. Star, J.F. Stoddart, D. Steuerman, M. Diehl, A. Boukai, E.W. Wong, X. Yang, S. Chung, H. Choi, J.R. Heath, Angew. Chem Int. Ed. 40 (2001) 1721.
[39] Y.K. Kang, O.-S. Lee, P. Deria, S.H. Kim, T.-H. Park, D.A. Bonnell, J.G. Saven, M.J. Therien, Nano Lett. 9 (2009) 1414.
[40] J. Liu, M.C. Hersam, MRS Bull. 35 (2010) 315.
[41] S.M. Bachilo, M.S. Strano, C. Kittrell, R.H. Hauge, R.E. Smalley, R.B. Weisman, Science 298 (2002) 2361.
[42] V.K. Sangwan, A. Behnam, V.W. Ballarotto, M.S. Fuhrer, A. Ural, E.D. Williams, App. Phys. Lett. 97 (2010) 043111.
[43] C.S. Smithson, S. Zhu, T. Wigglesworth, Y. Wu, Chem. Commun. 49 (2013) 8791.
[44] E.S. Snow, J.P. Novak, P.M. Campbell, D. Park, Appl. Phys. Lett. 82 (2003) 2145.
[45] T. Lei, J.-H. Dou, J. Pei, Adv. Mater. 24 (2012) 6457.
[46] G. Kim, S.-J. Kang, G.K. Dutta, Y.-K. Han, T.J. Shin, Y.-Y. Noh, et al., J. Am. Chem. Soc. 136 (2014) 9477.
[47] P. Sonar, S.P. Singh, Y. Li, Z.-E. Ooi, T. Ha, I. Wong, et al., Energy Environ. Sci. 4 (2011) 2288.